Chapter 6
Dolphin Echolocation Optimization

6.1 Introduction

Nature has provided inspiration for most of the man-made technologies. Scientists believe that dolphins are the second to humans in smartness and intelligence. Echolocation is the biological sonar used by dolphins and several kinds of other animals for navigation and hunting in various environments. This ability of dolphins is mimicked in this chapter to develop a new optimization method. There are different metaheuristic optimization methods, but in most of these algorithms, parameter tuning takes a considerable time of the user, persuading the scientists to develop ideas to improve these methods. Studies have shown that metaheuristic algorithms have certain governing rules and knowing these rules helps to get better results. Dolphin echolocation (DE) takes advantages of these rules and outperforms many existing optimization methods, while it has few parameters to be set. The new approach leads to excellent results with low computational efforts [1].

Dolphin echolocation is a new optimization method which is presented in this chapter. This method mimics strategies used by dolphins for their hunting process. Dolphins produce a kind of voice called *sonar* to locate the target; doing this dolphin changes sonar to modify the target and its location. Dolphin echolocation is depicted in Fig. 6.1. This fact is mimicked here as the main feature of the new optimization method.

6.2 Dolphin Echolocation in Nature

The term "echolocation" was initiated by Griffin [2] to describe the ability of flying bats to locate obstacles and preys by listening to echoes returning from high-frequency clicks that they emitted. Echolocating animals include some mammals

A. Kaveh, *Advances in Metaheuristic Algorithms for Optimal Design of Structures*,
DOI 10.1007/978-3-319-46173-1_6

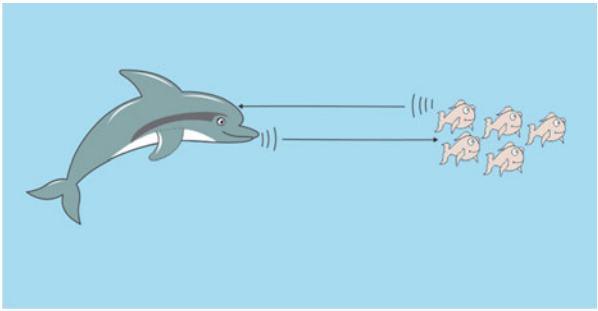

Fig. 6.1 A real dolphin catching its prey [1]

and a few birds. The best studied echolocation in marine mammals is that of the bottlenose dolphins, (Au [3]).

A dolphin is able to generate sounds in the form of clicks. Frequency of these clicks is higher than that of the sounds used for communication and differs between species. When the sound strikes an object, some of the energy of the sound wave is reflected back toward the dolphin. As soon as an echo is received, the dolphin generates another click. The time lapse between click and echo enables the dolphin to evaluate the distance from the object; the varying strength of the signal as it is received on the two sides of the dolphin's head enables him to evaluate the direction. By continuously emitting clicks and receiving echoes in this way, the dolphin can track objects and home in on them (May [4]). The clicks are directional and are for echolocation, often occurring in a short series called a click train. The click rate increases when approaching an object of interest [3].

Though bats also use echolocation, however, they differ from dolphins in their sonar system. Bats use their sonar system at short ranges of up to approximately 3–4 m, whereas dolphins can detect their targets at ranges varying from a few tens of meters to over a hundred meters. Many bats hunt for insects that dart rapidly to-and-fro, making it very different from the escape behavior of a fish chased by dolphin. The speed of sound in air is about one fifth of that of water, thus the information transfer rate during sonar transmission for bats is much shorter than that of the dolphins. These and many other differences in environment and prey require totally different types of sonar system, which naturally makes a direct comparison difficult [3, 5].

6.3 Dolphin Echolocation Optimization

6.3.1 Introduction to Dolphin Echolocation

Regarding an optimization problem, it can be understood that echolocation is similar to optimization in some aspects; the process of foraging preys using echolocation in dolphins is similar to finding the optimum answer of a problem.

As mentioned in the previous part, dolphins initially search all around the search space to find the prey. As soon as a dolphin approaches the target, the animal restricts its search and incrementally increases its clicks in order to concentrate on the location.

The method simulates dolphin echolocation by limiting its exploration proportional to the distance from the target. For making the relationship more clear, consider an optimization problem. Two stages can be identified: in the first stage the algorithm explores all around the search space to perform a global search, therefore it should look for unexplored regions. This task is carried out by exploring some random locations in the search space, and in the second stage it concentrates on investigation around better results achieved from the previous stage. These are obvious inherent characteristics of all metaheuristic algorithms. An efficient method is presented in Ref. [6] for controlling the value of the randomly created answers in order to set the ratio of the results to be achieved in phase 1 to phase 2.

By using dolphin echolocation (DE) algorithm, the user would be able to change the ratio of answers produced in phase 1 to the answers produced in phase 2 according to a predefined curve. In other words, global search changes to a local one gradually in a user-defined style.

The user defines a curve on which the optimization convergence should be performed, and then the algorithm sets its parameters in order to be able to follow the curve. The method works with the likelihood of occurrence of the best answer in comparison to the others. In other words, for each variable there are different alternatives in the feasible region; in each loop the algorithm defines the possibility of choosing the best-so-far achieved alternative according to the user-determined convergence curve. By using this curve, the convergence criterion is dictated to the algorithm, and then the convergence of the algorithm becomes less parameter dependent. The curve can be any smooth ascending curve, but there are some recommendations for it, which will be discussed later.

Previously it has been shown that there is a unified method for parameter selection in metaheuristics [6]. In the latter paper, an index called the convergence factor was presented. A *convergence factor* (*CF*) is defined as the average possibility of the elitist answer. As an example, if the aim is to devote some steel profiles to a structure that has four elements, then in the first step, frequency of modal profile of each element should be defined. *CF* is the mean of these frequencies. Table 6.1 illustrates an example of calculating the *CF* for a structure containing four elements.

6.3.2 Dolphin Echolocation Algorithm

Before starting optimization, the search space should be sorted using the following rule:

Table 6.1 An example for calculation of the *CF* [6]

	Element 1	Element 2	Element 3	Element 4
Answer 1	5	41	22	15
Answer 2	3	36	22	17
Answer 3	4	39	25	16
Answer 4	3	42	22	17
Answer 5	3	41	22	19
Modal answer	3	41	22	17
Frequency of the modal answer	3	2	4	2
Proportion of the modal answer among all answers	60 %	40 %	80 %	40 %
CF	55 %			

Search Space Ordering For each variable to be optimized during the process, sort alternatives of the search space in an ascending or descending order. If alternatives include more than one characteristic, perform ordering according to the most important one. Using this method, for variable j, vector A_j of length LA_j is created which contains all possible alternatives for the jth variable putting these vectors next to each other, as the columns of a matrix, the $Matrix\ Alternatives_{MA*NV}$ is created, in which MA is $\max(LA_j)_{\ j=1:NV}$; with NV being the number of variables.

Moreover, a curve according to which the convergence factor should change during the optimization process should be assigned. Here, the change of CF is considered to be according to the following curve:

$$PP(Loop_i) = PP_1 + (1 - PP_1)\frac{Loop_i^{Power} - 1}{(Loops\,Number)^{Power} - 1} \tag{6.1}$$

PP: Predefined probability

PP_1: Convergence factor of the first loop in which the answers are selected randomly

$Loop_i$: Number of the current loop

Power: Degree of the curve. As it can be seen, the curve in Eq. (6.1) is a polynomial of *Power* degree.

Loops number: Number of loops in which the algorithm should reach to the convergence point. This number should be chosen by the user according to the computational effort that can be afforded for the algorithm.

Figure 6.2 shows the variation of PP by the changes of the *Power*, using the proposed formula, Eq. (6.1).

The flowchart of the algorithm is shown in Fig. 6.3. The main steps of dolphin echolocation (DE) for discrete optimization are as follows:

1. Initiate NL locations for a dolphin randomly.
   This step contains creating L_{NL*NV} matrix, in which NL is the number of locations and NV is the number of variables (or dimension of each location).

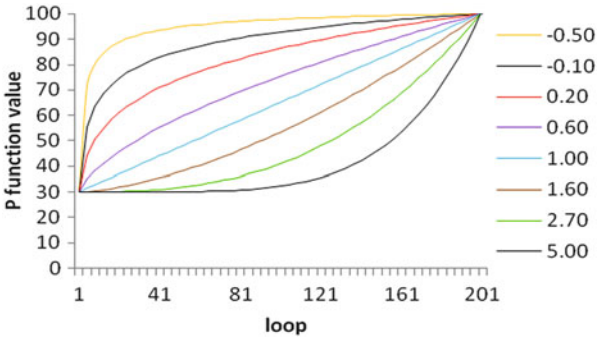

Fig. 6.2 Sample convergence curves, using Eq. (6.1) for different values for power [6]

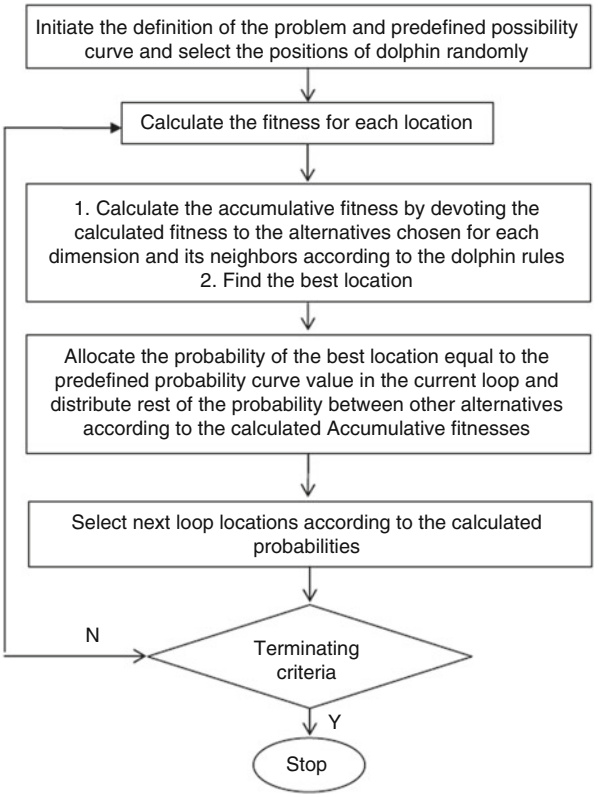

Fig. 6.3 The flowchart of the DE algorithm [1]

2. Calculate the *PP* of the loop using Eq. (6.1).
3. Calculate the fitness of each location.
   Fitness should be defined in a manner that the better answers get higher values. In other words the optimization goal should be to maximize the fitness.
4. Calculate the accumulative fitness according to dolphin rules as follows:
   (a) for $i = 1$ to the number of locations

for $j = 1$ to the number of variables
find the position of $L(i,j)$ in jth column of the alternatives matrix and name it as A.
for $k = -R_e$ to R_e

$$AF_{(A+k)j} = \frac{1}{R_e} * (R_e - |k|) Fitness(i) + AF_{(A+k)j} \tag{6.2}$$

end
end
end
where
$AF_{(A+k)j}$ is the accumulative fitness of the $(A + k)$th alternative (numbering of the alternatives is identical to the ordering of the Alternatives matrix) to be chosen for the jth variable and R_e is the effective radius in which accumulative fitness of the alternative A's neighbors is affected from its fitness. This radius is recommended to be not more than 1/4 of the search space; *Fitness* (i) is the fitness of location i.
It should be added that for alternatives close to edges (where $A + k$ is not a valid; $A + k < 0$ or $A + \mathrm{k} > LA_j$), the AF is calculated using a reflective characteristic. In this case, if the distance of an alternative to the edge is less than R_e, it is assumed that the same alternative exists where picture of the mentioned alternative can be seen, if a mirror is placed on the edge.

(b) In order to distribute the possibility much evenly in the search space, a small value of ε is added to all the arrays as $AF = AF + \varepsilon$. Here, ε should be chosen according to the way the fitness is defined. It is better to be less than the minimum value achieved for the fitness.

(c) Find the best location of this loop and name it "The best location." Find the alternatives allocated to the variables of the best location, and let their AF be equal to zero.
In other words:
for $j = 1$: number of variables
for $i = 1$: number of alternatives
if $i =$ the best location(j)

$$AF_{ij} = 0 \tag{6.3}$$

end
end
end

5. For variable $\mathrm{j}_{(\mathrm{j}=1 \text{ to NV})}$, calculate the probability of choosing alternative $\mathrm{i}_{(\mathrm{i}=1 \text{ to ALj})}$, according to the following relationship:

$$P_{ij} = \frac{AF_{ij}}{\sum_{i=1}^{\mathrm{LA_j}} AF_{ij}} \tag{6.4}$$

6. Assign a probability equal to PP to all alternatives chosen for all variables of the best location and devote rest of the probability to the other alternatives according to the following formula:
for $j = 1$: number of variables
for $i = 1$: number of alternatives
if $i =$ the best location(j)

$$P_{ij} = PP \tag{6.5}$$

Else

$$P_{ij} = (1 - PP)P_{ij} \tag{6.6}$$

end
end
end
Calculate the next step locations according to the probabilities assigned to each alternative.
Repeat Steps 2 to 6 as many times as the *loops number*.

Parameters of the Algorithm Input parameters for the algorithm are as follows:

(a) Loops number
For an optimization algorithm it is beneficial for the user to be able to dictate the algorithm to work according to the affordable computational cost. The answers may obviously be dependent on the selected number of loops and will improve by an increase in the loops number. However, the point is that one may not achieve results as bad as those of other optimization algorithms gained in less loops, because in this case although the algorithm quits its job much sooner than expected, the answer is good because of convergence criteria being reached. The number of loops can be selected by sensitivity analysis when high accuracy is required; however, in structural optimization of normal buildings, the loops number is recommended to be more than 50.

(b) Convergence curve formula
This is another important parameter to be selected for the algorithm. The curve should reach to the final point of 100 % smoothly. If the curve satisfies the abovementioned criteria, the algorithm will perform the job properly, but it is recommended to start with a linear curve and try the curves that spend more time (more loops) in high values of the PP. For example, if one is using proposed curves of this chapter, it is recommended to start with $Power = 1$

which usually gives good results, and it is better to try some cases of the $Power < 1$ to check if it improves the results.

(c) Effective radius (R_e)
This parameter is better to be chosen according to the size of search space. It is recommended to be selected less than ¼ of the size of the search space.

(d) ε
This parameter is better to be less than any possible fitness.

(e) Number of locations (NL)
This parameter is the same as the population size in GA or number of ants in ACO. It should be chosen in a reasonable way.

An Illustrative Numerical Example As an example consider the following simple mathematical function optimization problem:

$$\min\left(h = \sum_{i=1}^{N} x_i^2\right), \quad x_i \in Z, \ -20 \le x_i \le 20 \tag{6.7}$$

Considering $N = 4$, dolphin echolocation algorithm suggests the following steps:

Before starting the optimization process for the changes of CF, a curve should be selected using Eq. (6.1), utilizing Power = 1, the loops number = 8, and $PP1 = 0.1$ as follows:

$$PP = 0.1 + 0.9\left(\frac{Loop_i - 1}{7}\right) = 0.1 + 0.9(Loop_i - 1) \tag{6.8}$$

It should be noted that the $PP1$ is better to be considered as the CF of the randomly selected generation of the first loop, which is equal to 0.11 for this example.

Dolphin echolocation steps to solve the problem are as follows:

1. Create the initial locations randomly, which includes generating NL vectors consisting of N integer numbers between −20 and 20. For example, considering NL and N equal to 30 and 4, 30 vectors of length 4 should be selected randomly. One possible answer for the ith location can be $L_i = \{-10,4, -7,18\}$.
2. Calculate the PP of the loop using Eq. (6.8).
3. Calculate fitness for each location. In this example as the objective function is defined by Eq. (6.7), for the considered location (L_i), $h = (-10)^2 + 4^2 + (-7)^2 + 18^2 = 489$. As in DE, the fitness is used to calculate the probability. Better fitness values should have higher possibilities, then we can use $Fitness = 1/h$. It should be added that, for this special case, as h can be equal to zero, small value of 1 is added to the h in order to prevent the error of dividing by zero. Then the $Fitness = 1/(h + 1)$, and for the considered location $Fitness(L_i) = 1/(489 + 1) = 0.00204$.

4. Calculate the accumulative fitness, using Eq. (6.2). As discussed before the alternatives should be sorted in an ascending order. The $Alternatives_{MA*NV}$ (MA is the number of alternatives, and NV is the number of optimization variables) is allocated to the possible alternatives for variables. For this example, the Alternatives matrix is:

$$Alternatives = \begin{bmatrix} -20 & -20 & -20 & -20 \\ -19 & -19 & -19 & -19 \\ . & . & . & . \\ . & . & . & . \\ . & . & . & . \\ 19 & 19 & 19 & 19 \\ 20 & 20 & 20 & 20 \end{bmatrix} \tag{6.9}$$

Then for sample location, L_i, considering $R_e = 10$, Eq. (6.2) becomes:
for $i = L_i$
for $j = 1$ to 4
find the position of $L(i,j)$ in the jth column of the Alternatives matrix and name it as A.
for $k = -10$ to 10

$$AF_{(A+k)j} = \frac{1}{10} * (10 - |k|) Fitness(L_i) + AF_{(A+k)j} \tag{6.10}$$

end
end
end
Equation (6.10) can also be stated as:
for $j = \{1,2,3,4\}$
$L(i,j) = \{-10{,}4, -7{,}18\}$, then $A = \{11{,}25{,}14{,}39\}$
for $k = -10$ to 10

$$\begin{aligned} AF_{(11+k)1} &= \frac{1}{10} * (10 - |k|) Fitness(L_i) + AF_{(11+k)1} \\ AF_{(25+k)2} &= \frac{1}{10} * (10 - |k|) Fitness(L_i) + AF_{(25+k)2} \\ AF_{(14+k)3} &= \frac{1}{10} * (10 - |k|) Fitness(L_i) + AF_{(14+k)3} \\ AF_{(39+k)4} &= \frac{1}{10} * (10 - |k|) Fitness(L_i) + AF_{(39+k)4} \end{aligned} \tag{6.11}$$

end
end
Considering ε as the worth possible fitness, it will be $\varepsilon = 1/(4 * 20^2)$ and then $AF = AF + 0.000625$.

In these equations, it can be seen that, for example, for $j=2$ (the second variable), for calculating the accumulative fitness, the search space should be divided into two regions: affected region (in effective radius) and not affected region. Choosing R_e equal to 10, alternatives with absolute distance to 4 (alternative 4 is chosen for the second variable) more than 10 ($x<-6$ and $x>14$) are considered not affected. Also in the affected area the accumulative fitness resulted from this sample location changes linearly in a way that its maximum appears in $x=4$. The accumulative fitness to be added for this alternative is:

$$AF_{(x+25)2} = AF_{(x+25)2} + \begin{cases} 0 & x < -6 \\ \dfrac{Fitness(Li)}{10}(x+6) & -6 < x \le 4 \\ \dfrac{Fitness(Li)}{10}(14-x) & 4 < x \le 14 \\ 0 & x > 14 \end{cases} \qquad (6.12)$$

$$AF = AF + 0.000625$$

Figure 6.4 shows the result of performing the explained process for all four variables of this location.

Performing Step 4 for all the randomly selected answers, the final accumulative fitness of the first loop is achieved.

5. For variable $j_{(j=1 \text{ to } 4)}$, calculate the probability of choosing alternative $i_{(i=1 \text{ to } 40)}$, according to the following relationship:

$$P_{ij} = \frac{AF_{ij}}{\sum_{i=1}^{40} AF_{ij}} \qquad (6.13)$$

and consequently the probability will be according to Figs. 6.5 and 6.6.

6. Figure 6.5 demonstrates the accumulative fitness of variables X1, X2, X3, and X4. The best location of the first loop is achieved by setting variables as X1 = −11, X2 = 3, X3 =4, and X4 = 4. On the other hand, according to Eq. (6.8), PP for the first loop is equal to 10 %. As a result all variables in

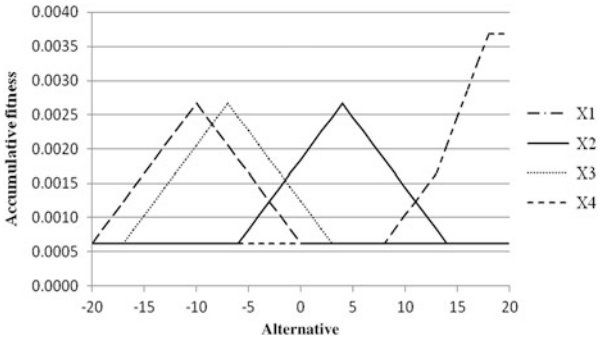

Fig. 6.4 Accumulative fitness resulted from sample location of the mathematical example [1]

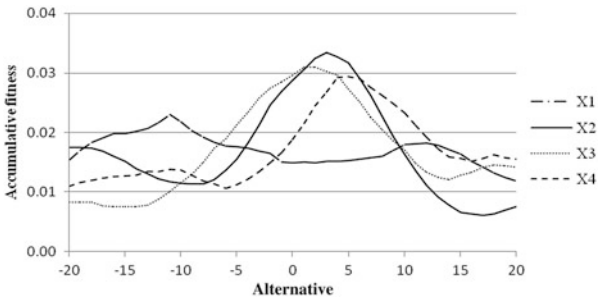

Fig. 6.5 Accumulative fitness of all four variables in the first loop of DE in mathematical example [1]

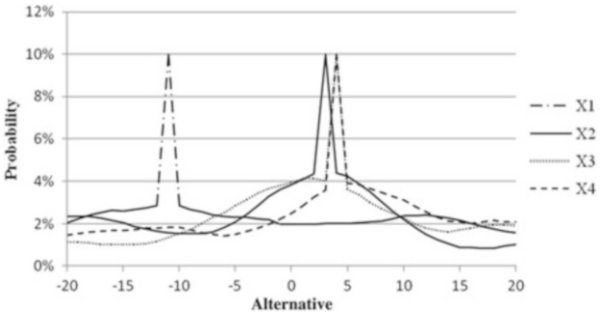

Fig. 6.6 Probability curve of all four variables in the first loop of DE in mathematical example [1]

their best placement are equal to 10 % probability of the other alternatives is defined distributing remaining value of probability equal to 90 % to the other alternatives, using the following formula:

$$P_{ij} = (1 - 0.1)P_{ij} = 0.9P_{ij} \tag{6.14}$$

Since the number of loops is equal to 8, Steps 2–6 should be repeated eight times. Figures 6.7, 6.8, 6.9, and 6.10 show the accumulative fitness and the probability of alternatives in loops 4 and 8, respectively. It can be seen from these figures that the probability changes in a way that in eight loops DE reaches the best answer.

Comparison Between the Dolphin Echolocation and Bat-Inspired Algorithm

Bat-inspired algorithm can be considered as a balanced combination of the standard particle swarm optimization and the intensive local search controlled by the loudness and pulse rate [7]. In this algorithm loudness and pulse frequency are echolocation parameters that gradually restrict the search according to pulse emission and loudness rules. This is while in dolphin echolocation algorithm, there is no movement to the best answer. DE algorithm works with probabilities.

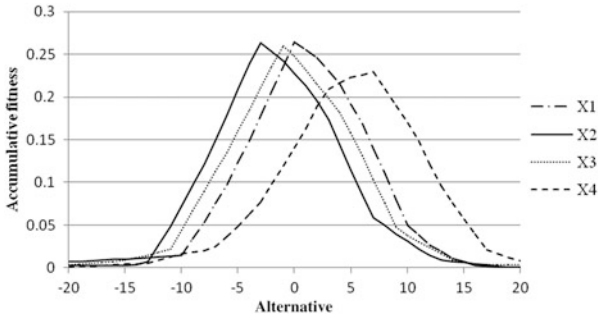

Fig. 6.7 Accumulative fitness of all four variables in the fourth loop of DE in of mathematical example [1]

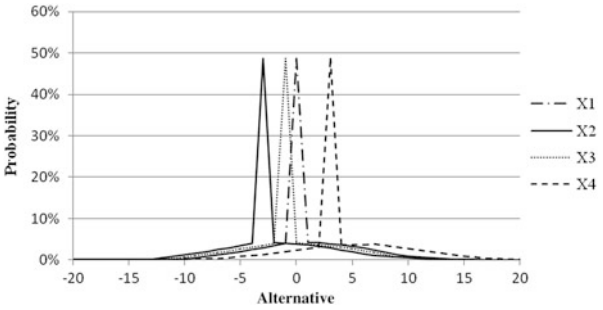

Fig. 6.8 Probability curve of all four variables in the fourth loop of DE in mathematical example

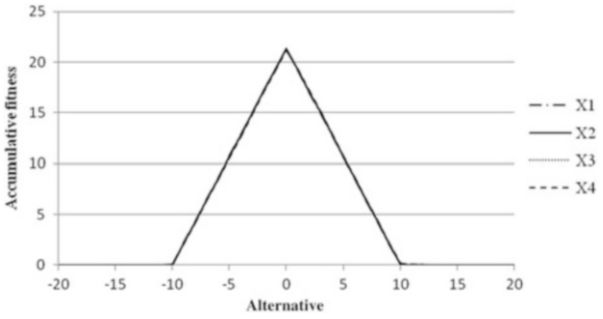

Fig. 6.9 Accumulative fitness of all four variables in the eighth loop of DE in of mathematical example [1]

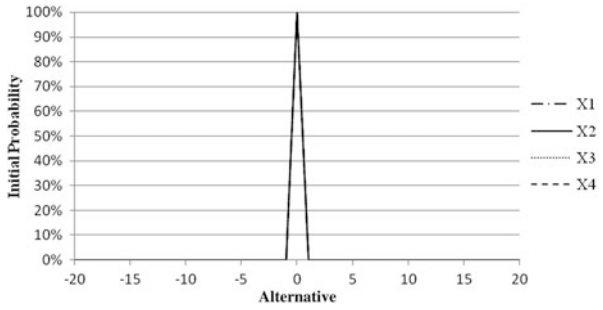

Fig. 6.10 Probability curve of all four variables in the eighth loop of DE in mathematical example [1]

6.4 Structural Optimization

In this study the structural optimization goal is to minimize the weight of the structure that is formulated as follows:

Minimize:

$$W = \rho \sum_{i=1}^{M} A_i L_i \tag{6.15}$$

Subjected to:

$$\begin{aligned} &KU - P = 0 \\ &g_1 \geq 0, g_2 \geq 0, \ldots, g_n \geq 0 \end{aligned} \tag{6.16}$$

where $g_1, g_2, \ldots, g_n$ are constraint functions depending on the element being used in each problem and K, U, and P are the stiffness matrix, nodal displacement, and nodal force vectors, respectively. In this study, different constraints are implemented for structural design including drift, displacement, and strength. Constraints are clarified in numerical examples.

Furthermore, such a constrained formulation is treated in an unconstrained form, using a penalized fitness function as:

$$F = F_0 - w^*\left(1 + K_p.V\right) \tag{6.17}$$

where F_0 is a constant taken as zero for the class of considered examples, K_p is the penalty coefficient, and V denotes the total constraints' violation considering all the load combinations.

6.5 Numerical Examples

In this section three trusses and two frames are optimized using the present algorithm, and the results are compared to those of some other existing approaches. The algorithms are coded in MATLAB, and structures are analyzed using the direct stiffness method.

6.5.1 Truss Structures

In the following three trusses are optimized, and the results of the present algorithm are compared to those of different algorithms.

6.5.1.1 A 25-Bar Spatial Truss

The 25-bar spatial truss structure shown in Fig. 6.11 has been studied in [8–11]. The material density is 0.1 lb/in^3 (2767.990 kg/m^3), and the modulus of elasticity is 10,000 ksi (68,950 MPa). The stress limitations of the members are ±40 kpsi (±275.80 MPa). All nodes in three directions are subjected to displacement limitations of ±0.35 inch (in) (±8.89 mm) imposed on every node in each direction. The structure includes 25 members, which are divided into eight groups as follows: (1) A_1, (2) A_2–A_5, (3) A_6–A_9, (4) A_{10}–A_{11}, (5) A_{12}–A_{13}, (6) A_{14}–A_{17}, (7) A_{18}–A_{21}, and (8) A_{22}–A_{25}. Two optimization cases are implemented.

Case 1: The discrete variables are selected from the set $D = \{0.01, 0.4, 0.8, 1.2, 1.6, 2.0, 2.4, 2.8, 3.2, 3.6, 4.0, 4.4, 4.8, 5.2, 5.6, 6.0\}$ (in^2) or {0.065, 2.58, 5.16, 7.74, 10.32, 12.90, 15.48, 18.06, 20.65, 23.22, 25.81, 28.39, 30.97, 33.55, 36.13, 38.71} (cm^2).

Case 2: The discrete variables are selected from the [12], listed in Table 6.2. The loads for both cases are shown in Table 6.3.

For solving this problem by the use of DE, the loops number is set to 80. Convergence curve is according to Eq. (6.1) considering $PP_1 = 0.15$ and $Power = 1$. R_e and ε are equal to 5 and 1, respectively.

According to Tables 6.4 and 6.5 and Fig. 6.12, DE achieves the best answer in approximately 50 loops in Case 1 and near 80 loops in Case 2, while HPSACO reaches to the same result in around 100 loops. It should be mentioned that Kaveh and Talatahari [11] show that the HPSACO itself has better convergence rate in comparison with GA, PSO, PSOPC, and HPSO.

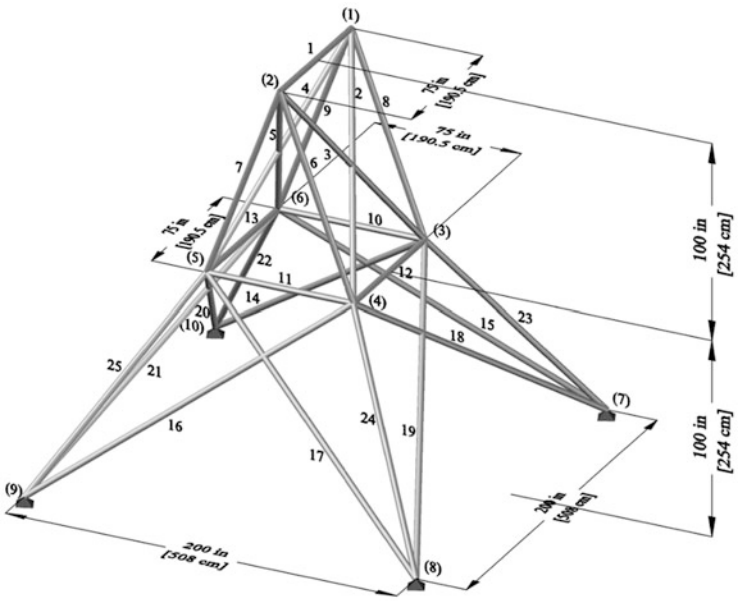

Fig. 6.11 Schematic of a 25-bar spatial truss

Table 6.2 The available cross-sectional areas of the AISC code

No.	in^2	mm^2	No.	in^2	mm^2
1	0.111	(71.613)	33	3.840	(2477.414)
2	0.141	(90.968)	34	3.870	(2496.769)
3	0.196	(126.451)	35	3.880	(2503.221)
4	0.250	(161.290)	36	4.180	(2696.769)
5	0.307	(198.064)	37	4.220	(2722.575)
6	0.391	(252.258)	38	4.490	(2896.768)
7	0.442	(285.161)	39	4.590	(2961.284)
8	0.563	(363.225)	40	4.800	(3096.768)
9	0.602	(388.386)	41	4.970	(3206.445)
10	0.766	(494.193)	42	5.120	(3303.219)
11	0.785	(506.451)	43	5.740	(3703.218)
12	0.994	(641.289)	44	7.220	(4658.055)
13	1.000	(645.160)	45	7.970	(5141.925)
14	1.228	(792.256)	46	8.530	(5503.215)
15	1.266	(816.773)	47	9.300	(5999.988)
16	1.457	(939.998)	48	10.850	(6999.986)
17	1.563	(1008.385)	49	11.500	(7419.430)
18	1.620	(1045.159)	50	13.500	(8709.660)
19	1.800	(1161.288)	51	13.900	(8967.724)
20	1.990	(1283.868)	52	14.200	(9161.272)
21	2.130	(1374.191)	53	15.500	(9999.980)
22	2.380	(1535.481)	54	16.000	(10,322.560)
23	2.620	(1690.319)	55	16.900	(10,903.204)
24	2.630	(1696.771)	56	18.800	(12,129.008)
25	2.880	(1858.061)	57	19.900	(12,838.684)
26	2.930	(1890.319)	58	22.000	(14,193.520)
27	3.090	(1993.544)	59	22.900	(14,774.164)
28	1.130	(729.031)	60	24.500	(15,806.420)
29	3.380	(2180.641)	61	26.500	(17,096.740)
30	3.470	(2238.705)	62	28.000	(18,064.480)
31	3.550	(2290.318)	63	30.000	(19,354.800)
32	3.630	(2341.931)	64	33.500	(21,612.860)

Table 6.3 Loading conditions for the 25-bar spatial truss

	Case 1			Case 2		
Node	P_X kips (kN)	P_Y kips (kN)	P_Z kips (kN)	P_X kips (kN)	P_Y kips (kN)	P_Z kips (kN)
1	0.0	20.0 (89)	−5.0 (22.25)	1.0 (4.45)	10.0 (44.5)	−5.0 (22.25)
2	0.0	−20.0 (89)	−5.0 (22.25)	0.0	10.0 (44.5)	−5.0 (22.25)
3	0.0	0.0	0.0	0.5 (2.22)	0.0	0.0
6	0.0	0.0	0.0	0.5 (2.22)	0.0	0.0

Table 6.4 Optimal design comparison for the 25-bar spatial truss (Case 1)

		Optimal cross-sectional areas (in^2)								
		Wu and Chow [8]	Lee and Geem [9]	Li et al. [10]			Kaveh and Talatahari [11] HPSACO		Present work [1]	
Element group		GA	HS	PSO	PSOPC	HPSO	in^2	cm^2	in^2	cm^2
1	A1	0.40	0.01	0.01	0.01	0.01	0.01	0.07	0.01	0.07
2	A2–A5	2.00	2.00	2.00	2.00	2.00	1.60	10.32	1.60	10.32
3	A6–A9	3.60	3.60	3.60	3.60	3.60	3.20	20.65	3.20	20.65
4	A10–A11	0.01	0.01	0.01	0.01	0.01	0.01	0.07	0.01	0.07
5	A12–A13	0.01	0.01	0.40	0.01	0.01	0.01	0.07	0.01	0.07
6	A14–A17	0.80	0.80	0.80	0.80	0.80	0.80	5.16	0.80	5.16
7	A18–A21	2.00	1.60	1.60	1.60	1.60	2.00	12.90	2.00	12.90
8	A22–A25	2.40	2.40	2.40	2.40	2.40	2.40	15.48	2.40	15.48
Weight (lb)		563.52	560.59	566.44	560.59	560.59	551.6	250.2 kg	551.6	250.2 kg

Table 6.5 Optimal design comparison for the 25-bar spatial truss (Case 2)

		Optimal cross-sectional areas (in^2)							
		Wu and Chow [8]	Li et al. [10]			Kaveh and Talatahari [11] HPSACO		Present work [1]	
Element group		GA	PSO	PSOPC	HPSO	in^2	cm^2	in^3	cm^3
1	A1	0.31	1.00	0.11	0.11	0.11	0.72	0.11	0.72
2	A2–A5	1.99	2.62	1.56	2.13	2.13	13.74	2.13	13.74
3	A6–A9	3.13	2.62	3.38	2.88	2.88	18.58	2.88	18.58
4	A10–A11	0.11	0.25	0.11	0.11	0.11	0.72	0.11	0.72
5	A12–A13	0.14	0.31	0.11	0.11	0.11	0.72	0.11	0.72
6	A14–A17	0.77	0.60	0.77	0.77	0.77	4.94	0.77	4.94
7	A18–A21	1.62	1.46	1.99	1.62	1.62	10.45	1.62	10.45
8	A22–A25	2.62	2.88	2.38	2.62	2.62	16.90	2.62	16.90
Weight (lb)		556.43	567.49	567.49	551.14	551.1	249.99	551.1	249.99

In addition, Fig. 6.13 shows the convergence factor history. It can be seen that the algorithm follows the predefined linear curve as expected.

6.5.1.2 A 72-Bar Spatial Truss

For the 72-bar spatial truss structure shown in Fig. 6.14, the material density is 0.1 lb/in^3 (2767.990 kg/m^3), and the modulus of elasticity is 10,000 ksi (68,950 MPa). The members are subjected to the stress limits of ±25 ksi (±172.375 MPa). The nodes are subjected to the displacement limits of ±0.25 in (±0.635 cm).

The 72 structural members of this spatial truss are sorted into 16 groups using symmetry: (1) A_1–A_4, (2) A_5–A_{12}, (3) A_{13}–A_{16}, (4) A_{17}–A_{18}, (5) A_{19}–A_{22}, (6) A_{23}–A_{30}, (7) A_{31}–A_{34}, (8) A_{35}–A_{36}, (9) A_{37}–A_{40}, (10) A_{41}–A_{48}, (11) A_{49}–A_{52}, (12) A_{53}–A_{54}, (13) A_{55}–A_{58}, (14) A_{59}–A_{66} (15), A_{67}–A_{70}, and (16) A_{71}–A_{72}.

Two optimization cases are implemented.

Case 1: The discrete variables are selected from the set $D = \{0.1, 0.2, 0.3, 0.4, 0.5, 0.6, 0.7, 0.8, 0.9, 1.0, 1.1, 1.2, 1.3, 1.4, 1.5, 1.6, 1.7, 1.8, 1.9, 2.0, 2.1, 2.2, 2.3, 2.4, 2.5, 2.6, 2.7, 2.8, 2.9, 3.0, 3.1, 3.2\}$ (in^2) or {0.65, 1.29, 1.94, 2.58, 3.23, 3.87, 4.52, 5.16, 5.81, 6.45, 7.10, 7.74, 8.39, 9.03, 9.68, 10.32, 10.97, 12.26, 12.90, 13.55, 14.19, 14.84, 15.48, 16.13, 16.77, 17.42, 18.06, 18.71, 19.36, 20.00, 20.65} (cm^2).

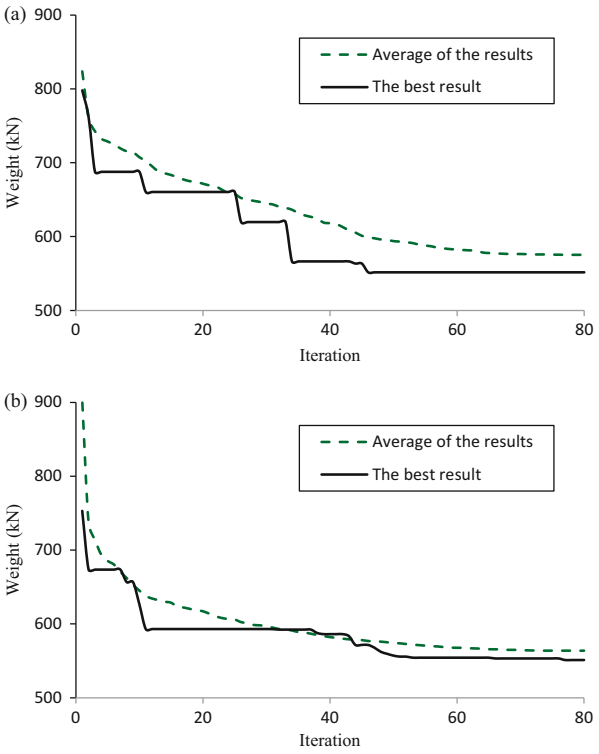

Fig. 6.12 The optimum answer convergence history for the 25-bar truss using DE [1]. (**a**) Case 1, (**b**) Case 2

Case 2: The discrete variables are selected from Table 6.2.

Table 6.6 lists the values and directions of the two load cases applied to the 72-bar spatial truss.

The problem has been solved by GA [8, 9] and DHPSO [11].

Solving the problem using DE, the loops number is set to 200. Convergence curve is according to Eq. (6.1) considering $PP_1 = 0.15$ and $Power = 1$. R_e and ε are equal to 5 and 1, respectively.

It can be seen from Table 6.7 that in Case 1 the best answer is achieved using DE that is better than GA and HS and although it is the same as DHPACO, but the penalty of the optimum answer is less than that of the DHPACO.

Moreover Table 6.8 shows that in Case 2, the DE achieves better results in comparison with the previously published works. Figure 6.15 shows that the DE can converge to the best answer in 200 loops and that it has a higher convergence rate compared to the other algorithms.

In addition, Fig. 6.16 shows the convergence factor history. It can be seen that the algorithm follows the predefined linear curve as expected.

Figure 6.17 shows the allowable and existing displacements for the nodes of the 72-bar truss structure using the DE.

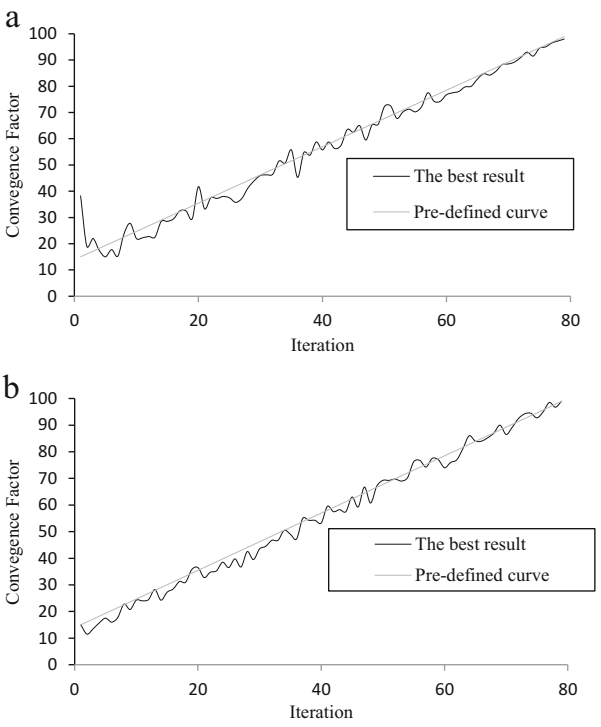

Fig. 6.13 The optimum answer and the average answers' convergence factor history for the 25-bar truss structure using the DE [1]. (**a**) Case 1, (**b**) Case 2

6.5.1.3 A 582-Bar Tower Truss

The 582-bar tower truss shown in Fig. 6.18 is chosen from Ref. [13]. The symmetry of the tower about x-axis and y-axis is considered to group the 582 members into 32 independent size variables.

A single load case is considered consisting of the lateral loads of 5.0 kN (1.12 kips) applied in both x and y directions and a vertical load of 30 kN (6.74 kips) applied in the z direction at all nodes of the tower. A discrete set of 140 economical standard steel sections selected from W-shape profile list based on area and radii of gyration properties is used to size the variables [13]. The lower and upper bounds on size variables are taken as 6.16 in^2 (39.74 cm^2) and 215.0 in^2 (1387.09 cm^2), respectively. The stress limitations of the members are imposed according to the provisions of ASD-AISC [12] as follows:

$$\begin{cases} \sigma_i^+ = 0.6Fy & for \quad \sigma_i \geq 0 \\ \sigma_i^- & for \quad \sigma_i < 0 \end{cases} \tag{6.18}$$

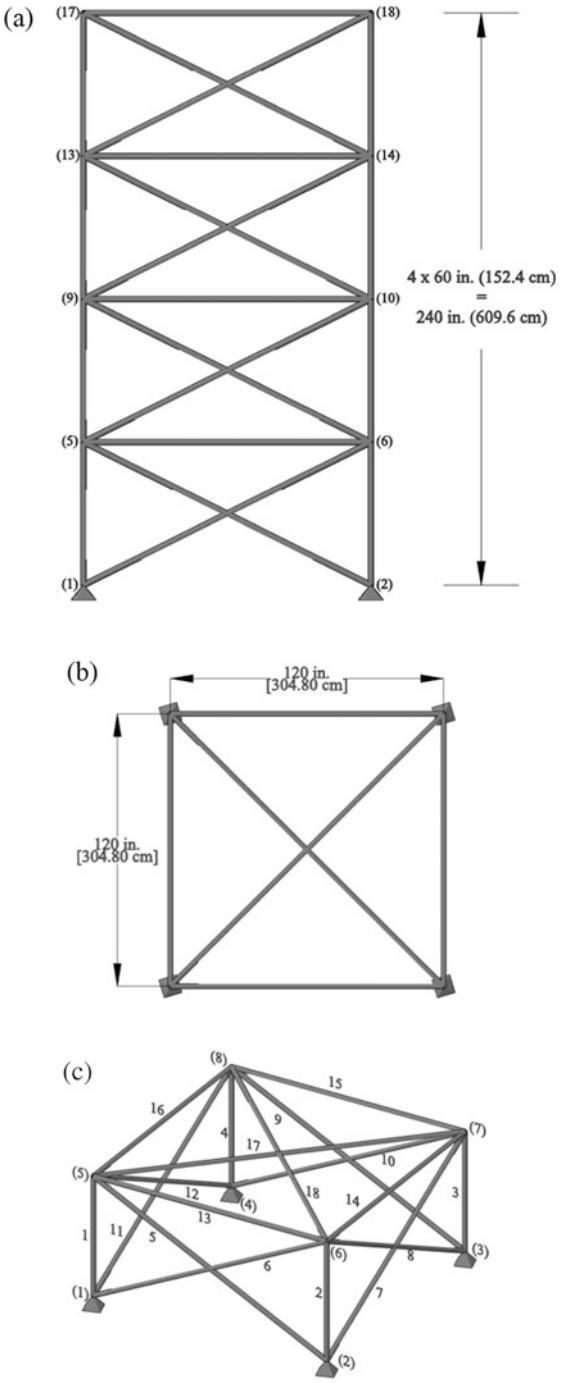

Fig. 6.14 Schematic of a 72-bar spatial truss [1]. (**a**) Front view, (**b**) top view, (**c**) element and node numbering system of a typical story

Table 6.6 Loading conditions for the 72-bar spatial truss

Node	Case 1			Case 2		
	P_x kips (kN)	P_Y kips (kN)	P_Z kips (kN)	P_X kips (kN)	P_Y kips (kN)	P_Z kips (kN)
17	5.0 (22.25)	5.0 (22.25)	−5.0 (22.25)	0	0	−5.0 (22.25)
18	0.0	0.0	0.0	0.0	0.0	−5.0 (22.25)
19	0.0	0.0	0.0	0.0	0.0	−5.0 (22.25)
20	0.0	0.0	0.0	0.0	0.0	−5.0 (22.25)

Table 6.7 Optimal design comparison for the 72-bar spatial truss (Case 1)

Element group		Optimal cross-sectional areas (in^2)					
		Wu and Chow [8]	Lee and Geem [9]	Kaveh et al. [11]		Present work [1]	
		GA	HS	DHPSACO		DE	
		in^2	in^2	in^2	cm^2	in^2	cm^2
1	A1–A4	1.5	1.9	1.9	12.26	2.0	12.90
2	A5–A12	0.7	0.5	0.5	3.23	0.5	3.23
3	A13–A16	0.1	0.1	0.1	0.65	0.1	0.65
4	A17–A18	0.1	0.1	0.1	0.65	0.1	0.65
5	A19–A22	1.3	1.4	1.3	8.39	1.3	8.39
6	A23–A30	0.5	0.6	0.5	3.23	0.5	3.23
7	A31–A34	0.2	0.1	0.1	0.65	0.1	0.65
8	A35–A36	0.1	0.1	0.1	0.65	0.1	0.65
9	A37–A40	0.5	0.6	0.6	3.87	0.5	3.23
10	A41–A48	0.5	0.5	0.5	3.23	0.5	3.23
11	A49–A52	0.1	0.1	0.1	0.65	0.1	0.65
12	A53–A54	0.2	0.1	0.1	0.65	0.1	0.65
13	A55–A58	0.2	0.2	0.2	1.29	0.2	1.29
14	A59–A66	0.5	0.5	0.6	3.87	0.6	3.87
15	A67–A70	0.5	0.4	0.4	2.58	0.4	2.58
16	A71–A72	0.7	0.6	0.6	3.87	0.6	3.87
Weight (lb)		400.66	387.94	385.54	174.9 kg	385.54	174.9 kg

where σ_i^- is calculated according to the slenderness ratio:

$$\sigma_i^- = \begin{cases} \left[\left(1 - \dfrac{\lambda_i^2}{2C_i^2}\right)F_y\right] \Big/ \left(\dfrac{5}{3} + \dfrac{5\lambda_i}{8C_C} - \dfrac{\lambda_i^3}{8C_C^3}\right) & for \quad \lambda_i < C_C \\ \dfrac{12\pi^2 E}{23\lambda_i^2} & for \quad \lambda_i \geq C_C \end{cases} \tag{6.19}$$

Table 6.8 Optimal design comparison for the 72-bar spatial truss (Case 2)

Element group		Optimal cross-sectional areas (in^2)				
		Wu et al. [8]	Kaveh et al. [11]		Present work [1]	
		GA	DHPSACO		DE	
		in^2	in^2	cm^2	in^2	cm^2
1	A1–A4	0.196	1.800	11.610	2.130	13.742
2	A5–A12	0.602	0.442	2.850	0.442	2.852
3	A13–A16	0.307	0.141	0.910	0.111	0.716
4	A17–A18	0.766	0.111	0.720	0.111	0.716
5	A19–A22	0.391	1.228	7.920	1.457	9.400
6	A23–A30	0.391	0.563	3.630	0.563	3.632
7	A31–A34	0.141	0.111	0.720	0.111	0.716
8	A35–A36	0.111	0.111	0.720	0.111	0.716
9	A37–A40	1.800	0.563	3.630	0.442	2.852
10	A41–A48	0.602	0.563	3.630	0.563	3.632
11	A49–A52	0.141	0.111	0.720	0.111	0.716
12	A53–A54	0.307	0.250	1.610	0.111	0.716
13	A55–A58	1.563	0.196	1.270	0.196	1.265
14	A59–A66	0.766	0.563	3.630	0.563	3.632
15	A67–A70	0.141	0.442	2.850	0.307	1.981
16	A71–A72	0.111	0.563	3.630	0.563	3.632
Weight (lb)		427.203	393.380	178.4 kg	391.329	177.47 kg

where E = the modulus of elasticity; F_y = the yield stress of A36 steel; $C_C = \sqrt{2\pi^2 E/F_y}$; λ_i = the slenderness ratio (kL_i/r_i); k = the effective length factor; L_i = the member length; and r_i = the radius of gyration. The other constraint is the limitation of the nodal displacements (no more than 8.0 cm or 3.15 in for each direction). In addition, the maximum slenderness ratio is limited to 300 for the tension members, and this limit is recommended to be 200 for the compression members according to the ASD-AISC [12] design code provisions.

The problem was solved later by Kaveh and Talatahari [14] and Sonmez [15]. Two cases for analyzing are used according to Ref. [15] as follows:

Case 1: All members are selected from a set of 140 W-shaped profiles according to Ref. [13], and the maximum number of evaluations is set to 50,000. For the DE, 25,000 evaluations are considered for this case to demonstrate the efficiency of the algorithm.

Case 2: There is no difference between Case 1 and Case 2 but in the number of evaluations which is set to 100,000. For the DE, 50,000 evaluations are considered for this case to demonstrate efficiency of the algorithm.

Convergence curve is according to Eq. (6.1) considering $PP_1 = 15\,\%$ and $Power = 0.2$. R_e and ε are equal to 10 and 1, respectively.

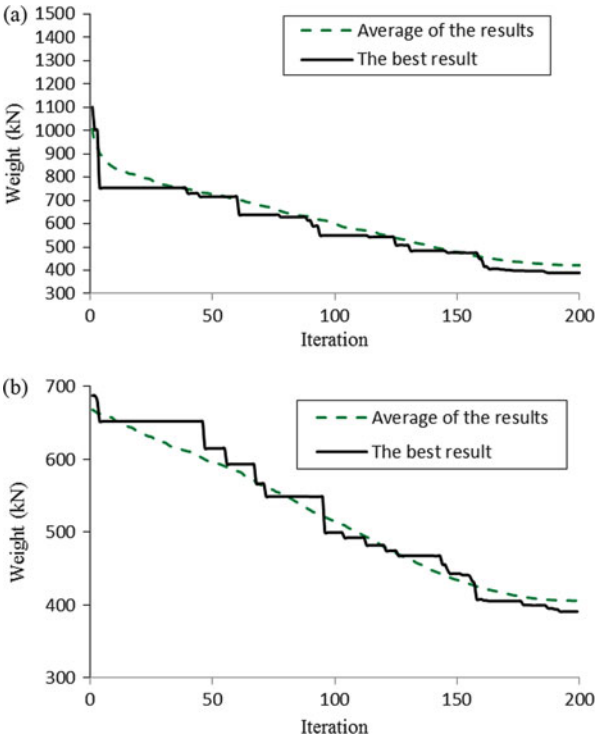

Fig. 6.15 The optimum answer and average answers' convergence history for the 72-bar truss using the DE [1]. (**a**) Case 1, (**b**) Case 2

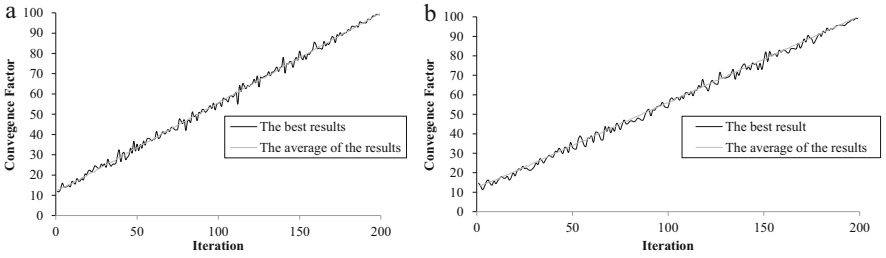

Fig. 6.16 The optimum answer and the average answers' convergence factor history for the 72-bar truss structure using the DE [1]. (**a**) Case 1, (**b**) Case 2

Results can be seen in Table 6.9, which shows that in Case 1, the DE outperforms the HPSACO, ABC, and PSO by 5.7 %, 2.3 %, and 1 %, respectively, and in Case 2, the DE result is 1.6% better than that of ABC algorithm. In addition comparing the results with those presented in [13], it can be seen that the optimum answer of the DE in Case 1 is 1.1, 1.3, 2.2, 2.7, 4.7, and 6.7 % lighter than those of the ESs, SA, TS, ACO, HS, and SGA.

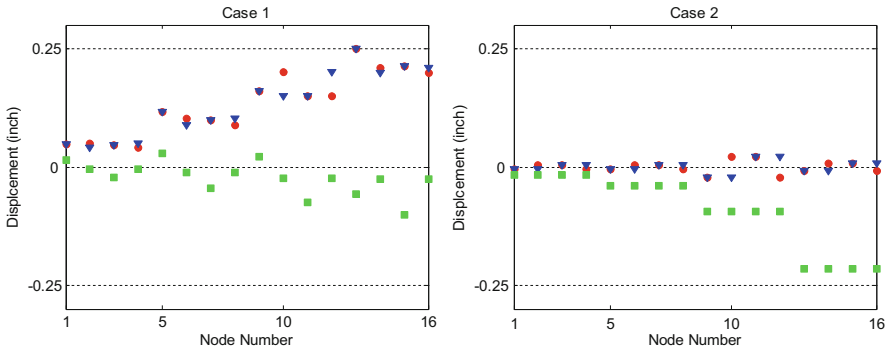

Fig. 6.17 Comparison of the allowable and existing displacements for the nodes of the 72-bar truss structure using the DE [1]

Figure 6.19 shows the comparison of the allowable and existing constrains for the 582-bar truss using the DE. The maximum values for displacement in x, y, and z directions are 3.148 in (7.995 cm), 2.986 in (7.584 cm), and 0.931 in (2.365 cm), respectively. The maximum stress ratio is 96.60 %. It can be seen that some displacements and stresses are near the boundary conditions. It should be mentioned that there is a small difference between analysis results of SAP2000 (Hasançebi et al. [13]), C# programming language code (Sonmez [15]), and MATLAB code (present study). Then checking the results of each code with another one may show a violation of constraints. Figure 6.19 shows that, according to the finite element program coded in MATLAB, there is no penalty for the best answer.

Figure 6.20 shows the convergence history of the best answer and average results for the DE, and Fig. 6.21 illustrates the convergence factor history. It can be seen that the algorithm follows the predefined linear curve as expected.

6.5.1.4 Frame Structures

The displacement and AISC combined strength constraints are the performance constraints of the frames as follows:

(a) Maximum lateral displacement:

$$\frac{\Delta_T}{H} < R \tag{6.20}$$

where Δ_T is the maximum lateral displacement of the structure (the roof lateral displacement), H is the height of the structure, and R is the maximum drift index.

(b) The inter-story displacements:

$$\frac{d_j}{h_j} < R_I, \quad j = 1, 2, \ldots, ns \tag{6.21}$$

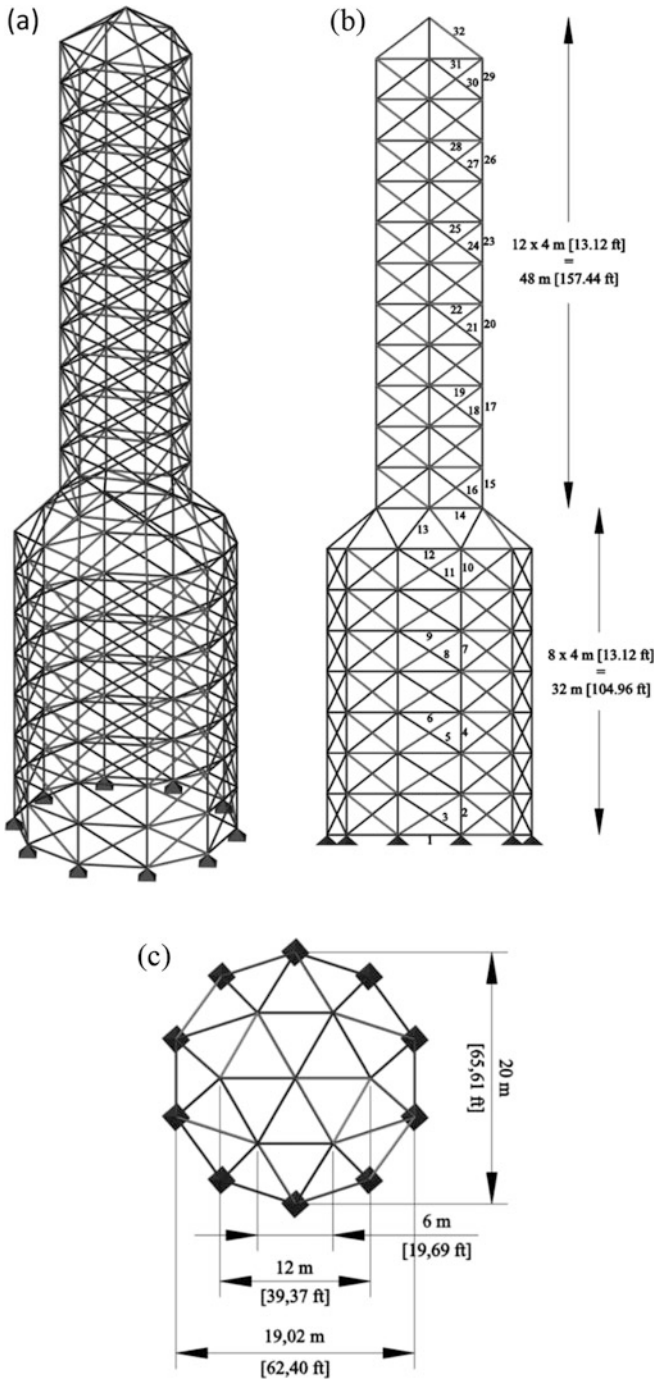

Fig. 6.18 Schematic of a 582-bar tower truss. (**a**) Three-dimensional view, (**b**) side view, (**c**) top view

Table 6.9 Optimal design comparison for the 582-bar spatial truss

	Optimal cross-section					
	Case 1				Case 2	
	Hasançebi et al. [13]	Sonmez [15]	Kaveh et al. [14]	Present work [1]	Sonmez [15]	Present work [1]
	(PSO)	(ABC)	(DHPSACO)	(DE)	(ABC)	(DE)
Element group	Ready section	Ready section	Ready section	Ready section	Ready section	Ready section
1	W8 × 21	W8 × 22	W8 × 24	W8 × 21	W8 × 22	W8 × 21
2	W12 × 79	W12 × 97	W12 × 72	W12 × 96	W10 × 78	W27 × 94
3	W8 × 24	W8 × 25	W8 × 28	W8 × 24	W8 × 25	W8 × 24
4	W10 × 60	W12 × 59	W12 × 58	W12 × 58	W14 × 62	W12 × 58
5	W8 × 24	W8 × 24	W8 × 24	W8 × 24	W8 × 24	W8 × 24
6	W8 × 21	W8 × 21	W8 × 24	W8 × 21	W8 × 21	W8 × 21
7	W14 × 48	W12 × 46	W10 × 49	W12 × 45	W12 × 51	W12 × 50
8	W8 × 24	W8 × 24	W8 × 24	W8 × 24	W8 × 24	W8 × 24
9	W8 × 21	W8 × 21	W8 × 24	W8 × 21	W8 × 21	W8 × 21
10	W10 × 45	W12 × 46	W12 × 40	W12 × 45	W10 × 50	W12 × 45
11	W8 × 24	W8 × 22	W12 × 30	W8 × 21	W8 × 25	W8 × 21
12	W10 × 68	W12 × 66	W12 × 72	W12 × 65	W10 × 69	W12 × 72
13	W14 × 74	W10 × 77	W18 × 76	W10 × 77	W18 × 77	W14 × 74
14	W14 × 48	W10 × 49	W10 × 49	W10 × 49	W14 × 49	W12 × 50
15	W18 × 76	W14 × 83	W14 × 82	W14 × 82	W10 × 78	W10 × 68
16	W8 × 31	W8 × 32	W8 × 31	W8 × 31	W8 × 32	W8 × 31
17	W16 × 67	W12 × 53	W14 × 61	W10 × 60	W21 × 62	W14 × 61
18	W8 × 24	W8 × 24	W8 × 24	W8 × 24	W8 × 24	W8 × 24
19	W8 × 21	W8 × 21	W8 × 21	W8 × 21	W8 × 21	W8 × 21
20	W8 × 40	W16 × 36	W12 × 40	W12 × 45	W14 × 43	W14 × 43
21	W8 × 24	W8 × 24	W8 × 24	W8 × 21	W8 × 24	W8 × 21
22	W8 × 21	W10 × 22	W14 × 22	W8 × 21	W8 × 21	W8 × 21
23	W10 × 22	W10 × 22	W8 × 31	W10 × 22	W8 × 24	W6 × 25
24	W8 × 24	W6 × 25	W8 × 28	W8 × 21	W8 × 24	W8 × 21
25	W8 × 21	W8 × 21	W8 × 21	W8 × 21	W8 × 21	W8 × 21
26	W8 × 21	W8 × 21	W8 × 21	W8 × 21	W8 × 21	W8 × 21
27	W8 × 24	W8 × 24	W8 × 24	W8 × 21	W8 × 24	W8 × 21
28	W8 × 21	W8 × 21	W8 × 28	W8 × 21	W8 × 21	W8 × 21
29	W8 × 24	W8 × 22	W16 × 36	W8 × 21	W8 × 21	W8 × 21
30	W8 × 21	W10 × 23	W8 × 24	W8 × 21	W8 × 21	W8 × 21
31	W8 × 21	W8 × 25	W8 × 21	W8 × 21	W8 × 24	W8 × 21
32	W8 × 24	W6 × 26	W8 × 24	W8 × 21	W8 × 24	W8 × 21
Best (lb)	363,795.7	368,484.1	380,982.7	360,367.8	365,906.3	360,143.3
Average (lb)	365,124.9	370,178.6	–	364,404.7	366,088.4	362,207.1
Worst (lb)	370,159.1	373,530.3	–	371,922.1	369,162.2	367,512.2
Evaluations (#)	50,000	50,000	8500	25,000	100,000	50,000
Differences compared to DE	0.95 %	2.25 %	5.72 %		1.60 %	

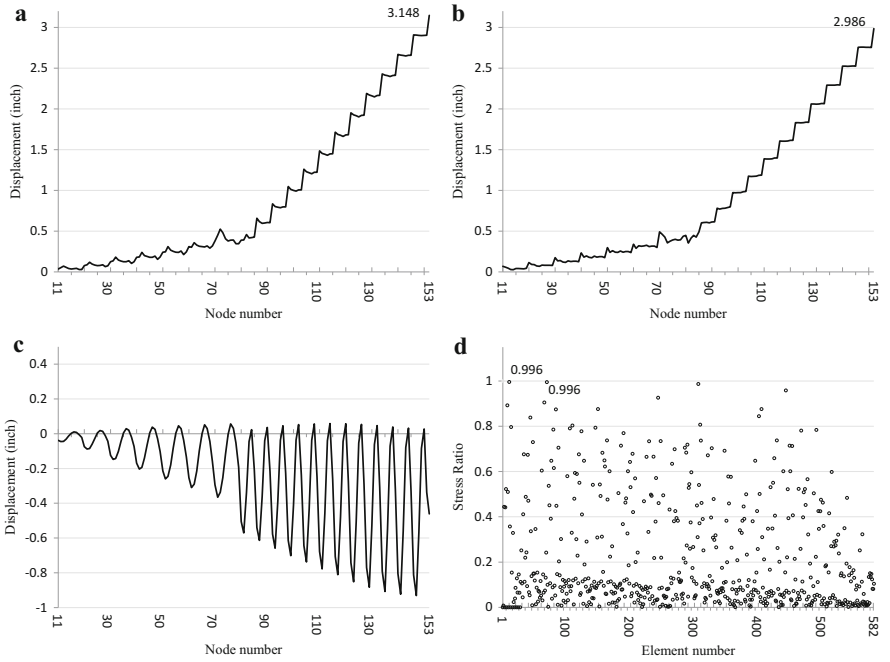

Fig. 6.19 Comparison of the allowable and existing constrains for the 582-bar truss, Case 2 using DE [1]. (**a**) Displacement in the x direction. (**b**) Displacement in y direction. (**c**) Displacement in the z direction. (**d**) Stress ratios

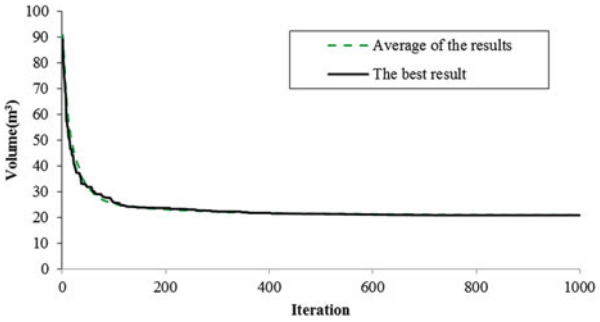

Fig. 6.20 Convergence history of optimum result and average results for the 582-bar tower truss, Case 2, using DE [1]

where d_j is the inter-story drift which is used to give the relative displacement of each roof in comparison to its following floor; h_j is the story height of jth floor; ns is the total number of stories; and R_I is the inter-story drift index which is equal to 1/300 according to the ANSI/AISC 360-05 (2005), Ref. [16].

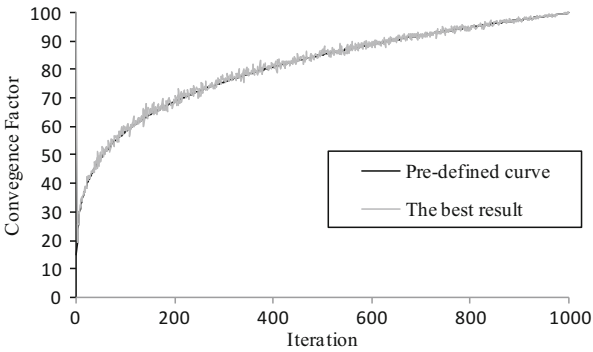

Fig. 6.21 Convergence factor history for the 582-bar tower truss [1], Case 2 using DE

(c) Element forces:

$$\begin{aligned} &\frac{P_u}{2\phi_C P_n}+\frac{M_u}{\phi_b M_n}<1 \quad for \quad \frac{P_u}{\phi_C P_n}<0.2 \\ &\frac{P_u}{\phi_C P_n}+\frac{8}{9}\frac{M_u}{\phi_b M_n}<1 \quad for \quad \frac{P_u}{\phi_C P_n}\geq 0.2 \end{aligned} \tag{6.22}$$

where P_u is the required strength (tension or compression); P_n is the nominal axial strength (tension or compression); ϕ_c is the axial resistance factor ($\phi_c = 0.9$ for tension, $\phi_c = 0.85$ for compression); M_u is required flexural strength; M_n is nominal flexural strength; and ϕ_b is the flexural resistance factor ($\phi_b = 0.9$).

6.5.1.5 A 3-Bay 15-Story Planar Frame

Figure 6.22 shows the configuration and applied loads of a 3-bay 15-story frame structure chosen from Ref. [14]. This frame consists of 64 joints and 105 members. The sway of the top story is limited to 23.5 cm. The material has a modulus of elasticity equal to $E = 200$ GPa and a yield stress of $F_y = 248.2$ MPa. The effective length factors of the members are calculated as $K_x \geq 0$ for a sway-permitted frame, and the out-of-plane effective length factor is specified as $K_y = 1.0$. Each column is considered as non-braced along its length, and the unbraced length for each beam member is specified as one-fifth of the span length.

For solving this problem by DE, the loops number is set to 100. The convergence curve is according to Eq. (6.1) considering $PP_1 = 0.15$ and $Power = 1$. R_e and ε are equal to 5 and 1, respectively.

Results of the present study and those of Refs. [7, 14], and [17] are provided in Table 6.10. It can be seen that the DE achieves results that are 26 %, 14 %, 8 %,6 %, and 4 % lighter than the PSO, PSOPC, HPSACO, ICA, and CSS, respectively.

Convergence history is depicted in Fig. 6.23. It can be seen that the present algorithm leads to the best answer in 100 loops which is less than that of the CSS (250 loops).

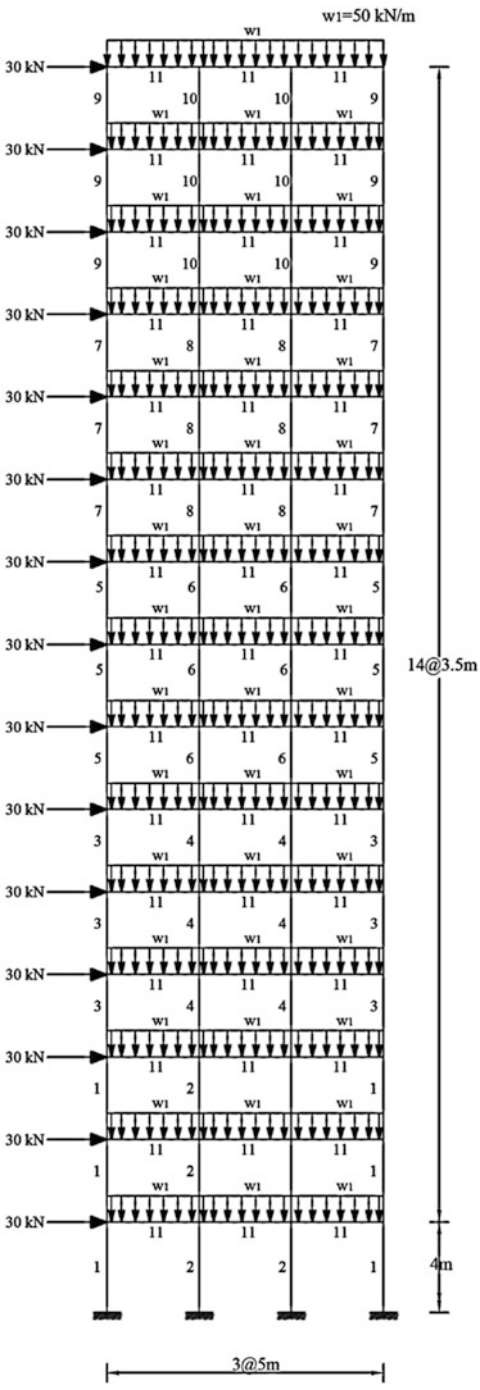

Fig. 6.22 Schematic of a 3-bay 15-story planar frame

Table 6.10 Optimal design comparison for the 3-bay 15-story planar frame

	Optimal W-shaped sections					
	Kaveh and Talatahari					Present work [1]
Element group	PSO [14]	PSOPC [14]	HPSACO [14]	ICA [17]	CSS [7]	
1	W33 × 118	W27 × 129	W21 × 111	W24 × 117	W21 × 147	W12 × 87
2	W33 × 263	W24 × 131	W18 × 158	W21 × 147	W18 × 143	W36 × 182
3	W24 × 76	W24 × 103	W10 × 88	W27 × 84	W12 × 87	W21 × 93
4	W36 × 256	W33 × 141	W30 × 116	W27 × 114	W30 × 108	W18 × 106
5	W21 × 73	W24 × 104	W21 × 83	W14 × 74	W18 × 76	W18 × 65
6	W18 × 86	W10 × 88	W24 × 103	W18 × 86	W24 × 103	W14 × 90
7	W18 × 65	W14 × 74	W21 × 55	W12 × 96	W21 × 68	W10 × 45
8	W21 × 68	W27 × 94	W27 × 114	W24 × 68	W14 × 61	W12 × 65
9	W18 × 60	W21 × 57	W10 × 33	W10 × 39	W18 × 35	W6 × 25
10	W18 × 65	W18 × 71	W18 × 46	W12 × 40	W10 × 33	W10 × 45
11	W21 × 44	W21 × 44	W21 × 44	W21 × 44	W21 × 44	W21 × 44
Weight (kN)	496.68	452.34	426.36	417.466	412.62	395.35
Differences compared to DE	26 %	14 %	8 %	6 %	4 %	

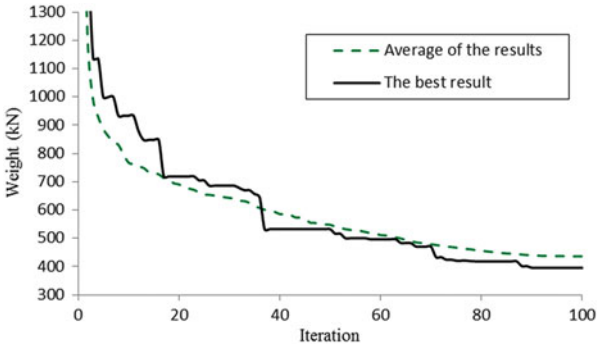

Fig. 6.23 The optimum answer and average answer with the convergence history for the 3-bay 15-story frame using the DE [1]

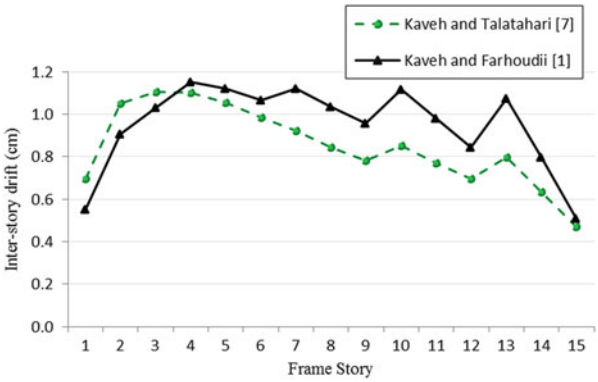

Fig. 6.24 Comparison of the allowable and the existing inter-story drift for the 3-bay 15-story planar frame [1]

The maximum value of displacement is 14.27 cm which is less than the allowable limit (23.5 cm).

Figure 6.24 shows the inter-story drifts, the maximum value of which is 1.15 cm. This is less than the allowable value (1.17 cm). It can be recognized that by reducing the weight of structure, its stiffness is reduced, and then the inter-story drifts are closer to the maximum allowable value.

In Fig. 6.25 the stress ratios of the elements are shown. The maximum stress ratio is 99.69 %. One can see that similar to the inter-story limitation, stress ratios are closer to the limit line.

Figure 6.26 shows the *CF* changes during optimization. It is clear that the *CF* changes around predefined line.

6.5.1.6 A 3-Bay 24-Story Planar Frame

Figure 6.27 shows the topology and the service loading conditions for a 3-bay 24-story frame consisting of 100 joints and 168 members which is chosen from Camp et al. [18]. The frame is designed following the LRFD specification and uses

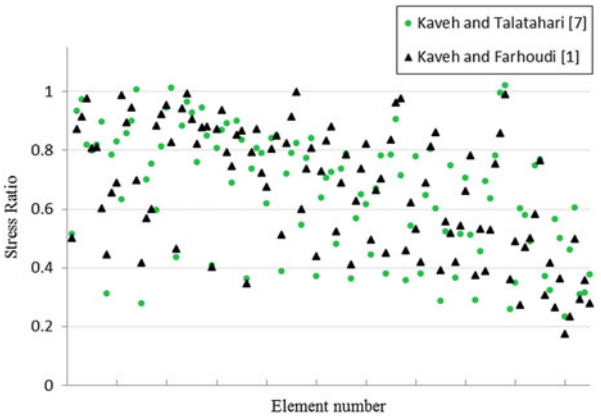

Fig. 6.25 Comparison of the allowable and the existing stress ratios for the 3-bay 15-story planar frame [1]

Fig. 6.26 The optimum answer and the average answer with the convergence factor history for the 3-bay 15-story planar frame using the DE [1]

an inter-story drift displacement constraint. The material properties are a modulus of elasticity equal to $E = 205$ GPa and a yield stress of $F_y = 230.3$ MPa.

The effective length factors of the members are calculated as $K_x \geq 0$ for the sway-permitted frame, and the out-of-plane effective length factor is specified as $K_y = 1.0$. All columns and beams are considered non-braced along their lengths. Fabrication conditions are imposed on the construction of the 168-element frame requiring that the same beam section be used in the first and third bay on all the floors except the roof beams, resulting in four beam groups.

Beginning at the foundation, the exterior columns are combined into one group, and the interior columns are combined together in another group over three consecutive stories. The grouping results in 16 column sections and four beam sections for a total of 20 design variables. In this example, each of the four beam element groups is chosen from all 267 W-shapes, while the 16 column element groups are limited to W14 sections (37 W-shapes).

For solving this problem by the DE, the loops number is set to be equal to 200. The convergence curve is according to Eq. (6.1) considering $PP_1 = 0.15$ and $Power = 1$. R_e and ε are equal to 5 and 1, respectively.

Results of the present study and those of Camp et al. [18], Degertekin [19], and Kaveh and Talatahari [7, 17, 20] are provided in Table 6.11. It can be seen that the

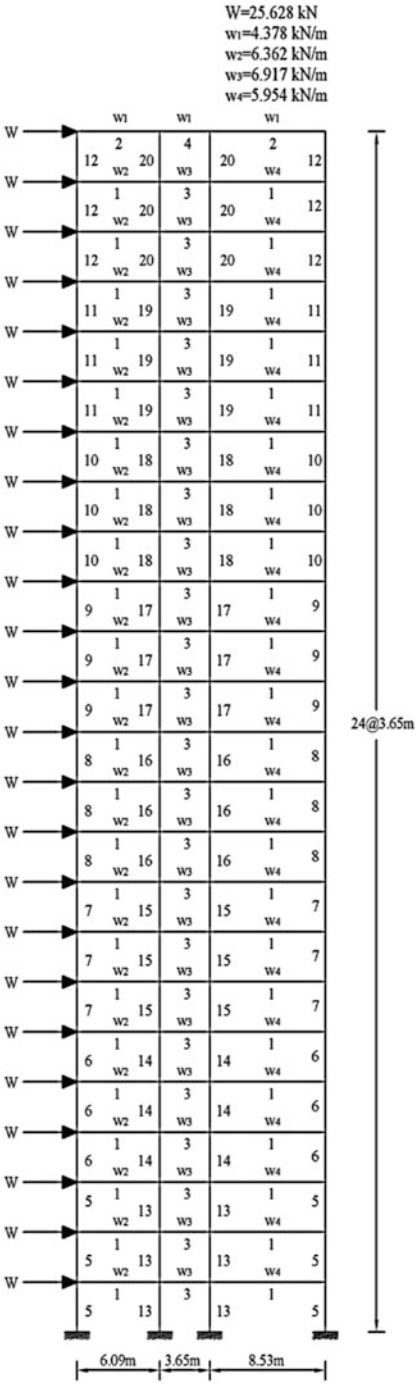

Fig. 6.27 Schematic of a 3-bay 24-story planar frame

Table 6.11 Optimal design comparison for the 3-bay 24-story planar frame

	Optimal W-shaped sections					
	Camp et al. [18]	Degertekin [19]	Kaveh and Talatahari			
Element group	ACO	HS	IACO [20]	ICA [17]	CSS [7]	Present work [1]
1	W30 × 90	W30 × 90	W30 × 99	W30 × 90	W30 × 90	W30 × 90
2	W8 × 18	W10 × 22	W16 × 26	W21 × 50	W21 × 50	W6 × 20
3	W24 × 55	W18 × 40	W18 × 35	W24 × 55	W21 × 48	W21 × 44
4	W8 × 21	W12 × 16	W14 × 22	W8 × 28	W12 × 19	W6 × 9
5	W14 × 145	W14 × 176	W14 × 145	W14 × 109	W14 × 176	W14 × 159
6	W14 × 132	W14 × 176	W14 × 132	W14 × 159	W14 × 145	W14 × 145
7	W14 × 132	W14 × 132	W14 × 120	W14 × 120	W14 × 109	W14 × 132
8	W14 × 132	W14 × 109	W14 × 109	W14 × 90	W14 × 90	W14 × 99
9	W14 × 68	W14 × 82	W14 × 48	W14 × 74	W14 × 74	W14 × 68
10	W14 × 53	W14 × 74	W14 × 48	W14 × 68	W14 × 61	W14 × 61
11	W14 × 43	W14 × 34	W14 × 34	W14 × 30	W14 × 34	W14 × 43
12	W14 × 43	W14 × 22	W14 × 30	W14 × 38	W14 × 34	W14 × 22
13	W14 × 145	W14 × 145	W14 × 159	W14 × 159	W14 × 145	W14 × 109
14	W14 × 145	W14 × 132	W14 × 120	W14 × 132	W14 × 132	W14 × 109
15	W14 × 120	W14 × 109	W14 × 109	W14 × 99	W14 × 109	W14 × 90
16	W14 × 90	W14 × 82	W14 × 99	W14 × 82	W14 × 82	W14 × 82
17	W14 × 90	W14 × 61	W14 × 82	W14 × 68	W14 × 68	W14 × 74
18	W14 × 61	W14 × 48	W14 × 53	W14 × 48	W14 × 43	W14 × 43
19	W14 × 30	W14 × 30	W14 × 38	W14 × 34	W14 × 34	W14 × 30
20	W14 × 26	W14 × 22	W14 × 26	W14 × 22	W14 × 22	W14 × 26
Weight (kN)	980.63	956.13	967.33	946.25	945.02	912.26
Difference compared to DE	7.5 %	4.8 %	6.0 %	3.7 %	3.6 %	

DE achieves results that are 7.5 %, 4.8 %,6 %, 3.7 %, and 3.6 % lighter than those of the ACO, HS, IACO, ICA, and CSS, respectively.

Convergence history is depicted in Fig. 6.28. It can be observed that DE leads to the best answer in 200 loops which is less than that of CSS being 275 loops.

The maximum value of displacement is 26.11 cm which is less than the allowable limit (29.20 cm).

Figure 6.29 shows the inter-story drifts with maximum value being 1.202 cm that is less than the allowable value (1.205 cm). It can be recognized that by reducing the weight of structure, its stiffness is reduced, and the inter-story drifts are quite close to the maximum allowable value.

In Fig. 6.30 the stress ratios of the elements are shown. One can see that similar to the inter-story limitation, the stress ratios are closer to the limitation line. The maximum stress ratio is 98.33 %.

Figure 6.31 shows the *CF* changes during the optimization process. It is clear that the *CF* changes around the predefined line.

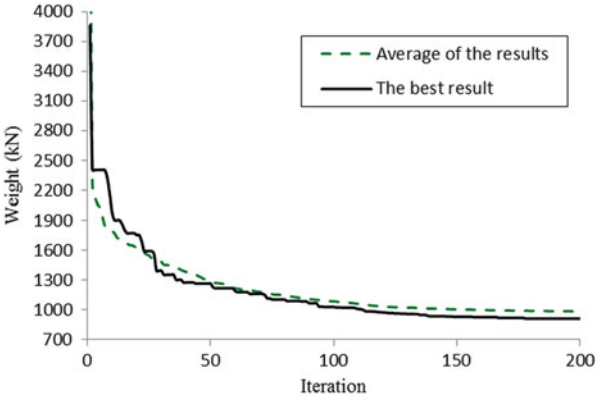

Fig. 6.28 The optimum answer and the average answer, with the convergence history for the 3-bay 24-story frame using the DE [1]

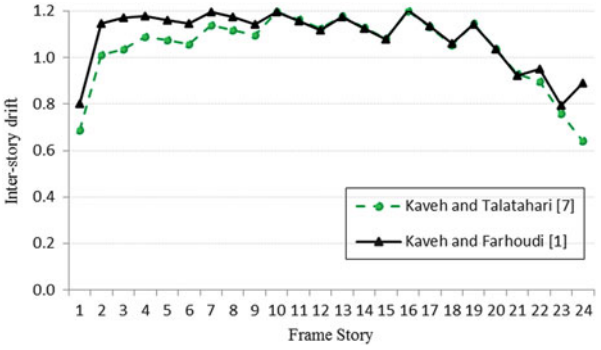

Fig. 6.29 Comparison of the allowable and the existing inter-story drift for the 3-bay 24-story planar frame [1]

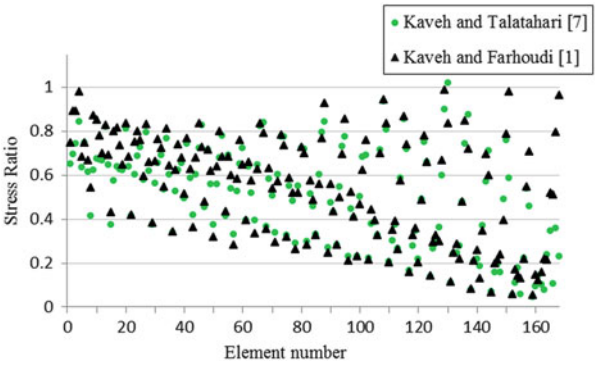

Fig. 6.30 Comparison of the allowable and existing stress ratio for the 3-bay 24-story planar frame [1]

Fig. 6.31 The optimum answer and the average answer with the convergence factor history for the 3-bay 24-story planar frame using the DE [1]

6.5.1.7 Discussion

In this study a novel optimization method is developed based on dolphin echolocation. The new method has the advantage of working according to the computational effort that user can afford for his/her optimization. In this algorithm, the convergence factor defined by Kaveh and Farhoudi [6] is controlled in order to perform a suitable optimization.

For the examples optimized in this chapter, the DE achieves better results with higher convergence rates compared to other existing metaheuristic algorithms such as GA, ACO, PSO, BB–BC, HS, ESs, SGA, TS, ICA, IACO, PSOPC, HPSACO, and CSS previously applied to these problems. The authors believe that the results achieved from metaheuristics are mostly dependent on the parameter tuning of the algorithms. It is also believed that by performing a limited number of numerical examples, one cannot correctly conclude the superiority of one method with respect to the others. Dolphin echolocation is an optimization algorithm that has the capability of adopting itself by the type of the problem in hand, having a reasonable convergence rate, and leading to an acceptable optimum answer in a number of loops specified by the user.

References

1. Kaveh A, Farhoudi N (2013) A new optimization method: dolphin echolocation. Adv Eng Softw 59:53–70
2. Griffin DR (1958) Listening in the dark: the acoustic orientation of bats and men. Yale University Press, New Haven, CT, p 413 [Biological Laboratories, Harvard University, Cambridge. MA]
3. Au WWL (1993) The sonar of dolphins. Springer, New York
4. May J (1990) The Greenpeace book of dolphins. Greenpeace Communications Ltd., London
5. Thomas JA, Moss CF, Vater M (2002) Echolocation in bats and dolphins. University of Chicago Press, Chicago, IL
6. Kaveh A, Farhoudi N (2011) A unified approach to parameter selection in meta-heuristic algorithms for layout optimization. J Constr Steel Res 67:15453–15462
7. Kaveh A, Talatahari S (2012) Charged system search for optimal design of planar frame structures. Appl Soft Comput 12:382–393
8. Wu SJ, Chow PT (1995) Steady-state genetic algorithms for discrete optimization of trusses. Comput Struct 56:979–991
9. Lee KS, Geem ZW, Lee SH, Bae KW (2005) The harmony search heuristic algorithm for discrete structural optimization. Eng Optim 37:663–684
10. Li LJ, Huang ZB, Liu F (2009) A heuristic particle swarm optimization method for truss structures with discrete variables. Comput Struct 87:435–443
11. Kaveh A, Talatahari S (2009) A particle swarm ant colony optimization for truss structures with discrete variables. Comput Struct 87:1129–1140
12. Construction (AISC) (1989) Manual of steel construction—allowable stress design, 9th edn. AISC, Chicago, IL
13. Hasançebi O, Çarbaş S, Doğan E, Erdal F, Saka MP (2009) Performance evaluation of metaheuristic search techniques in the optimum design of real size pin jointed structures. Comput Struct 87(5–6):284–302
14. Kaveh A, Talatahari S (2009) Hybrid algorithm of harmony search, particle swarm and ant colony for structural design optimization. Stud Comput Intell 239:159–198
15. Sonmez M (2011) Discrete optimum design of truss structures using artificial bee colony algorithm. Struct Multidiscip Optim 43:85–97
16. ANSI/AISC 360-05 (2005) Specification for structural steel buildings. American Institute of Steel Construction, Chicago, IL, 60601-1802, March 9
17. Kaveh A, Talatahari S (2010) Optimum design of skeletal structures using imperialist competitive algorithm. Comput Struct 88:1220–1229
18. Camp CV, Bichon J, Stovall SP (2005) Design of steel frames using ant colony optimization. J Struct Eng ASCE 131(3):369–379
19. Degertekin SO (2008) Optimum design of steel frames using harmony search algorithm. Struct Multidiscip Optim 36:393–401
20. Kaveh A, Talatahari S (2010) An improved ant colony optimization for design of planar steel frames. Eng Struct 32:864–876